ENERGY TRANSFER BETWEEN EXCITONS AND THE 3d-ELECTRONS OF Mn^{2+} IN $Zn_{1-x}Mn_xSe$

A THESIS SUBMITTED TO
THE SCHOOL OF GRADUATE STUDIES
ADDIS ABABA UNIVERSITY

IN PARTIAL FULFILLMENT
OF THE REQUIREMENTS FOR THE
DEGREE OF MASTER OF SCIENCE IN PHYSICS

by
AFRASH EJIGU

ADDIS ABABA, ETHIOPIA,
June, 1995

ACKNOWLEDGEMENT

I offer my deepest gratitude to my advisor Dr. U. Stutenbaumer for his frequent advice, kind encouragement and patience, and valuable comments and suggestions in guiding and supervising this work. His unreserved guidance in using computers is also acknowledged.

I wish to thank the Ministry of Education who granted me sponsorship to participate in the graduate program. I am also thankfull for the Graduate School Office and the Physics Department of the AAU for their material support.

I am grateful to all members of the Physics Department of the AAU who have delivered their unreserved cooperation throughout my stay.

Finally, special thanks is due to H. Zuber, at the Technical University Berlin, for providing me his data.

ABSTRACT

In this thesis the excitation spectra of the $^4T_1 \rightarrow {}^6A_1$ emission of Mn^{2+} in $Zn_{1-x}Mn_xSe$ crystals and their dependence on the crystal temperature, intensity of the exciting laser and manganese concentration ($x \leq 0.016$) are investigated. Eventhougth some of the excitation spectra of these crystals were published in literature the origin of one of the excitation band (M-band) still remains unknown. The M-band is an excitation band of the $^4T_1 \rightarrow {}^6A_1$ emission of Mn^{2+} in $Zn_{1-x}Mn_xSe$ within the spectral range of bound excitons. Computer fitting techniques were used to determine some important parameters of the M-band and the bound exciton band (BE-band).

From the comparison of the crystal temperature, exciting laser intensity and Mn concentration dependence of some of these fitting parameters of the M-band with that of the BE-band it is found that the M-band is built up of a multiple of bound excitons, which are different from that of the BE-band.

CONTENTS

LIST OF TABLES

LIST OF FIGURES

1. INTRODUCTION

Excitation spectra of the $^4T_1 \rightarrow {}^6A_1$ emission of Mn^{2+} in $Zn_{1-x}Mn_xSe$ crystals and their dependence on the crystal temperature, manganese concentration ($x \leq 0.016$) and intensity of the exciting laser gives evidence of an energy transfer between excitons and deep impurities. This energy transfer helps to know more about excitons (how they are built and their lifetimes) and impurities. $Zn_{1-x}Mn_xSe$ is a wide band gap semimagnetic semiconductor. It is a cubic crystal system for $x \leq 0.016$ [1].

The optical data for this work were obtained by excitation of $Zn_{1-x}Mn_xSe$ crystals. The data were collected by H. Zuber at the Technical University Berlin. Some of the excitation spectra of these crystals were published by U. Stutenbaumer et al [2]. But the origin of one of the excitation bands of the excitation spectra of the $Zn_{1-x}Mn_xSe$ crystals is yet unknown. The aim of this work is to determine the origin of the excitation band called M-band. The M-band is an excitation band between 2.70 eV and 2.76 eV at 4.2 K in the excitation spectra of the $^4T_1 \rightarrow {}^6A_1$ emission of Mn^{2+} in $Zn_{1-x}M_xSe$ crystal in the spectral range of bound excitons. The unknown M-band is analyzed using computer fitting methods. This fitting gives the band width, the area and center of this band as parameters and their dependence on temperature, excitation intensity and manganese concentration. Some of these fitting parameters of the M-band were compared with that of the bound exciton band (BE-band) to investigate the origin of the M-band.

After this brief introduction, the second chapter introduces the basic concepts of exciton, free-exciton and bound exciton. In the third chapter previous works on excitons and energy transfer between excitons and the 3d-electrons of Mn^{2+} ions in II-VI compounds (ZnS, CdS and ZnSe) are presented. These works gave experimental evidence for the existence of excitons and the energy transfer between excitons and the 3d-electrons of Mn^{2+} ions in II-VI compounds using excitation spectroscopy.

In the fourth chapter curve fitting is introduced as a method of analyzing our excitation spectra. The data for this work are taken from the chi-square fitting parameters of the excitation spectra of Mn^{2+} and DAP emissions in $Zn_{1-x}Mn_xSe$ crystals, and these data are interpreted into figures. In the fifth chapter the figures are discussed to account for the origin of the M-band.

2. EXCITON MODEL

2.1 Excitons

When a semiconductor is illuminated with light, the photons may be absorbed or they may propagate through the semiconductor depending on the photon energy (hν) and on the energy gap (E_g).

When $h\nu > E_g$ the photon can interact with a valence electron and elevate the electron into the conduction band thereby creating a free electron-hole pair. The hole is a quasi-particle with positive charge, wave vector and the spin vector are opposite to those of the electron which has been removed from the valence band.

Reflectance and absorption spectra often show a structure for photon energies just below the energy gap, where we might expect the crystal to be transparent. This structure is caused by the absorption of a photon with the creation of a bound electron-hole pair, the coulomb interaction being responsible for the binding energy (see fig. 2.1).The bound electron-hole pair is called an exciton. Exciton is used here to signify the modification of the absorption rates of photons due to coulomb interaction between the electron and the valence band hole.

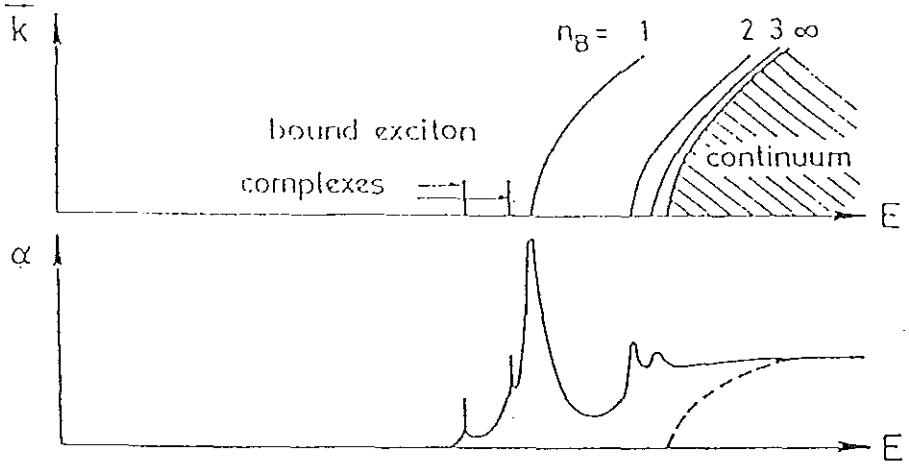

Fig. 2.1. Effect of an exciton level on optical absorption of a semiconductor. α is the absorption coefficient and n_B is the main quantum number for energy states of free excitons [3]

An exciton can move through the crystal and transport energy, it does not transport charge since it is electrically neutral. All excitons are unstable with respect to the ultimate recombination process in which the electron drops into the hole. Excitons can also form complexes such as biexciton from two excitons.

2.2 Free (Mott-Wannier) excitons

The Mott-Wannier model begins with an electron in the conduction band and a hole in the valence band which are bound weakly to each other by the coulomb force. This exciton overlaps many atoms in the crystal and does not resemble the excitation of any constituent atom. The dielectric screening of the crystal serves to weaken the attraction between electron and hole, and thus to increase their average separation. The Mott-Wannier model is therefore most appropriate for materials with a high dielectric constant.

Since free excitons occur frequently in solids let us see its quantitative treatment. Here the electron and the hole are spatially separated. The dominant contribution to the electron-hole interaction is the coulomb attraction between the electron and the hole. This is the long-range contribution. We assume that conduction and valence bands are isotropic, parabolic and degenerate only with respect to +/-k, and that the maximum of the valence band and the minimum of the conduction band occur at $K = 0$, i.e. at the Γ-point. With this assumption, we may use the effective mass approximation; m^*_e and m^*_h are the effective masses of the electron and the hole respectively. The properties of the free excitons in the limit of this idealized band structure is given by the so called hydrogenic model characterized by the main quantum number n_B. In this model, the possible energy states of free exciton $E_{FE}(n_B , K)$ are essentially the Bohr eigenstates:

$$E_{FE}(n_B, K) = E_g - R^*_y \frac{1}{n_B^2} + \frac{h^2 k^2}{2M} \quad ; n_B = 1,2,3,... \qquad (2.1)$$

where $M = m^*_e + m^*_h$ = translational mass of the exciton.

E_g = band gap at k =0.

K = wave vector of the center-of-mass motion.

With the modified Rydberg energy R^*_y given by [4]

$$R^*_y = \frac{\mu e^4}{2h^2\varepsilon^2} = 13.6\, eV \frac{\mu}{\varepsilon^2} \qquad (2.2a)$$

where $\mu = m^*_e m^*_h / (m^*_e + m^*_h)$ = reduced effective mass of the exciton.

ε = dielectric constant.

The energy gap (E_g) appears as an additive term because the zero of energy is placed at the top of the valence band edge. Because the exciton can move almost freely in the crystal, the kinetic energy of the center-of-mass must also be included in the energy of the exciton third term in eq. (2.1). The second term in eq. (2.1) is called the binding energy of the free exciton series (E^b_{FE})

$$E^b_{FE} = \frac{\mu e^4}{2h^2\varepsilon^2 n_B^2} \qquad (2.3)$$

From the great analogy to the hydrogen atom, the Bohr-radius (a_B) of the $n_B = 1$ ground state is

$$a_B = \frac{h^2 \varepsilon}{\mu e^2} \qquad (2.4a)$$

Typical values of R_y^* in semiconductors are

$$1.0 \text{ meV} \leq R_y^* \leq 200 \text{ meV} \qquad (2.2b)$$

The Bohr-radius of the $n_B = 1$ ground state is ranging

$$5\,\mathring{A} \leq a_B \leq 200\,\mathring{A} \qquad (2.4b)$$

This means that ' a_B ' is generally considerably larger than the lattice constant. The Mott-Wannier exciton is a weakly bound electron-hole pair in which the electron and the hole are separated by distances large compared with the lattice constant. The energy spectrum of this type of exciton consists of a series of parabolic energy curves converging to the ionization limit E_g (see fig. 2.2b).

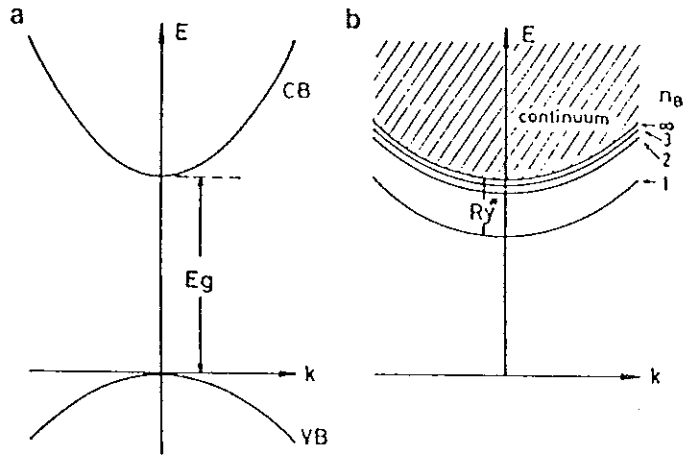

Fig. 2.2. Band structure (a) and energy spectra of excitons (b) for an idealized band gap semiconductor [5].

Since the energetic separation of the exciton state from the band edge ' E_g ' is rather small, measurements show that the excitonic character of optical absorption must be carried out at very low temperatures for materials with high dielectric constant and low effective

mass. This is because the exciton binding energy given by eq. (2.3) is very much less than the thermal energy k_BT, and the exciton levels can not be distinguished from the conduction band at high temperatures. In an optical absorption measurements, one sees only exciton states with $|K| \approx 0$, since light quanta can only transfer a negligibly small momentum.

2.3 Bound excitons

The discussion of energy transfer in semiconductors has so far been limited to intrinsic aspects. But even the purest semiconductor available still contain about 10^{15} - 10^{16} imperfections per cm^3. By intentional doping this number can be increased by several orders of magnitude. Excitons bound and localized at some defect or impurity are called bound excitons. Impurities like isoelectronic trap (I), neutral acceptors (A^o), neutral donors (D^o), charged donors (D^+) and charged acceptors (A^-) may bind an electron-hole pair forming a bound exciton complex (BEC). The binding energy of the exciton to the complex is decreasing from IX complexes over A^oX and D^oX to D^+X and A^-X. The A^-X complex is generally unbound, i.e., it is for this BEC energetically more favorable to form a neutral acceptor and a free electron [5].

Depending on the number of created free excitons per unit volume, bound exciton complex is build up by successive capture of free excitons at neutral impurities. A complex consisting of m bound excitons and characterized by the complex numbers ' m ' can increase by capture of another free exciton (FE) thus becoming an (m+1) complex, it may decrease by the decay of one exciton resulting in a complex with (m-1) bound particles. The energy of a bound exciton (E_{BEC}) is given by [6].

$$E_{BEC} = E_{FE} - E^b_{BE} = E_g - E^b_{FE} - E^b_{BE} \qquad (2.5)$$

where E_{FE} = energy of free exciton.

E^b_{BE} = binding energy of an exciton to the complex.

From eq. (2.5) we can see that the energy of bound exciton, like the energy of free exciton, depends on the band gap energy. Hence both the energy levels of free excitons and that of bound excitons are affected linearly with the thermal shift of the band gap energy.

Besides the capture of free excitons by impurities or defects, bound exciton complexes in their electronic ground or excited states can be formed directly by resonant optical excitation.

A bound exciton state in a E (k) diagram is represented by a horizontal line. Obviously, it is a type of oscillator without spatial dispersion. The singlet states of the BEC are generally coupling to the electromagnetic field. The oscillator strength per impurity atom of a BEC is considerably larger as compared to the oscillator strength per unit cell of free excitons. On the other hand, the density of the impurity centers in "pure" materials is several orders of magnitude smaller than that of unit cells, resulting in moderate values of absorption coefficient [5].

$$10\ cm^{-1} \leq \alpha_{BEC} \leq 10^{3}\ cm^{-1}$$

$$10^{4} cm^{-1} \leq \alpha_{FE} \leq 10^{6} cm^{-1} \qquad (2.6)$$

There are many optical phenomena connected with BEC, which have an analogous with the optical properties of free exciton-polaritons.* For example, they can act as virtually excited intermediate states in Raman scattering, or they can give luminescence without emission of phonons or under emission of one or several optical phonons.

*The quantum of the coupled exciton-polariton wave field is called exciton-polariton.

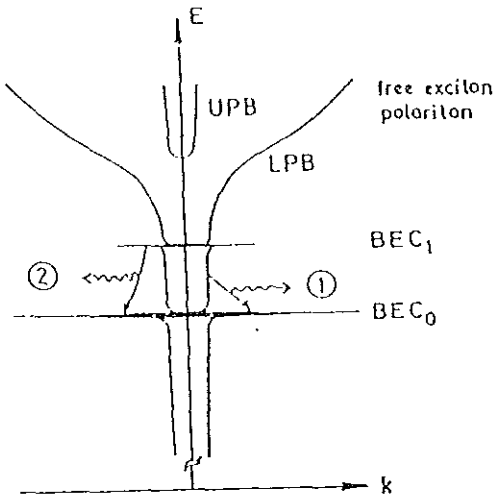

Fig. 2. 3. Dispersion for a free exciton-polariton and a bound exciton complex [5].

The excited states of BEC can be described in terms of energy transfer. In fig. 2.3 the dispersion of the lower polariton branch (LPB) together with two energy levels of a BEC, the lower one being the ground state the upper one the excited state, is shown. If a spectrally narrow tunable laser-beam ($\hbar\omega_i$) is sent on the sample, it will be absorbed if $\hbar\omega_i = E_{BEC0}$. In addition, strong light scattering (or resonance-fluorescence) occurs.

For $\hbar\omega_i > E_{BEC0}$, polaritons on the LPB are created. They may relax to a small extent by acoustic phonon emission to the BEC_0 producing some luminescence in this spectral region (process 1). If $\hbar\omega_i = E_{BEC1}$ a large number of BEC_1 will be created. They relax to BEC_0 by transferring energy, e.g. to the acoustic phonon system (process 2). As a result, a peak appears in a plot of the BEC_0-luminescence intensity as a function of $\hbar\omega_i$ for constant excitation intensity whenever $\hbar\omega_i$ falls on an optically allowed excited state of the BEC[7].

2.4 Donor-acceptor pair luminescence

Donor-acceptor pair (DAP) luminescence in II-VI compounds results from the recombination of an electron bound to a donor with a hole bound to an acceptor.

If a semiconductor, containing donors and acceptors, at low temperature is irradiated with photons of energy greater than the band gap, the light induced electron-hole pairs will neutralize the ionized donors and acceptors present in the sample [8]. If the localized wavefunctions of electrons and holes of the D^o and A^o complexes overlap at least a little bit, the electron-hole pair may recombine under the emission of a photon.

3. ENERGY TRANSFER BETWEEN EXCITONS AND IMPURITIES IN II-VI COMPOUND CRYSTALS

Here previous works on excitons and energy transfer between excitons and the 3d-electrons of Mn^{2+} ions in II-VI compounds (ZnS, CdS and ZnSe) are presented. These works gave experimental evidence for the existence of excitons and the energy transfer between excitons and the 3d-electrons of Mn^{2+} ions in II-VI compounds using excitation spectroscopy.

3.1 Luminescence excitation spectra and their exciton structures of ZnS phosphors

Hoshina and Kawi [9] investigated the excitation spectra of hexagonal $Zn_{1-x}Mn_xS$ at 75 K for $x = 10^{-4}$, prepared by firing precipitated ZnS powder at 1200 °C in a sulfur atmosphere for 2 hours in a quartz tube followed by quenching the tube into water. A 150 W Xe lamp was used as the exciting light source.

They for the first time clearly showed that the Mn center in ZnS can bind an intrinsic exciton. This fact follows from the exciton lines exhibited by excitation spectra for Mn^{2+} luminescence. The exciton lines in their excitation spectra are denoted by A_1 , B_1 , and C_1. The notations distinguish the three valence band maxima to which the holes of the excitons belong. A_1 , B_1 and C_1 lines occur at 3.864 eV, 3.891 eV and 3.989 eV respectively, at 75 K (see fig. 3.1).

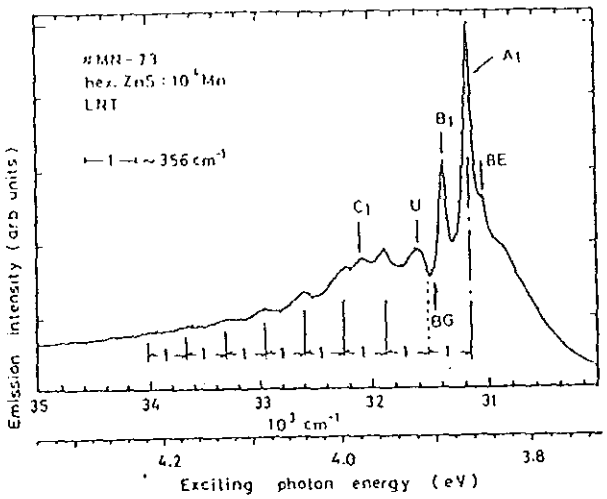

Fig. 3.1. Excitation spectra for Mn luminescence in hexagonal $Zn_{1-x}Mn_xS$ ($x = 10^{-4}$) at T = 75 K [9].

The Mn center in $Zn_{1-x}Mn_xS$ is considered to act as isoelectronic hole trap. The probable excitation mechanisms of Mn^{2+} ion in ZnS is shown in fig. 3.2. ' I ' indicates the isoelectronic Mn center.

Model 1. A free exciton is bound to a Mn center to form a bound exciton around it. Subsequent recombination of the bound exciton promotes the Mn^{2+} ion to an excited state by resonant energy transfer.

Model 2. A hole is first trapped by a Mn center, and then a free electron is attracted by the positive charge to form a bound exciton, which is followed by resonant transfer of the exciton recombination energy to Mn^{2+}. The Mn luminescence under band gap excitation may be due mainly to such a mechanism.

Model 3. The hole trapped by a Mn center, and recombines with an electron bound to a donor, if donors are present in the neighborhood. The recombination energy is transferred to the Mn center.

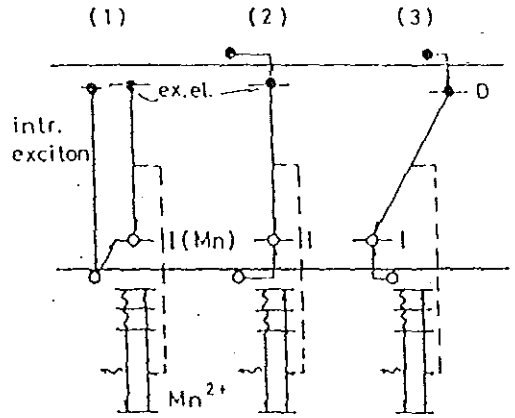

Fig. 3.2. Models for excitation mechanisms of Mn^{2+} ion in $Zn_{1-x}Mn_xS$ [9].

3.2 Dependence of energy gap on x and temperature in $Zn_{1-x}Mn_xSe$

Bylsma et al. *[1]* carried out photoluminescence (PL) and reflectivity measurements on $Zn_{1-x}Mn_xSe$, and investigated the PL and reflectivity data near the band-edge to determine the band gap as a function of Mn concentration (x) and temperature for $0 \leq x \leq 0.554$ and $8\ K \leq T \leq 300\ K$. The crystals used were grown by the Bridgman method. The excitation source for PL measurements was an argon-ion laser operated in the UV (351.1nm - 363.8nm) lines. Reflection spectra were made in a back scattering configuration. The incident light was selected from a 150 W Xenon arc lamp.

The photoluminescence spectra of $Zn_{1-x}Mn_xSe$ for $0 \leq x \leq 0.554$ at 6.5 K is shown in fig. 3.3. The spectrum of pure ZnSe ($x = 0$) is typical of those seen by other investigators. The commonly observed near-edge emission is dominated by a peak at 2.704 eV and followed by vibronically coupled side bands. This emission has been attributed to transitions involving holes bound to acceptors and either free electrons or electrons bound to donors.

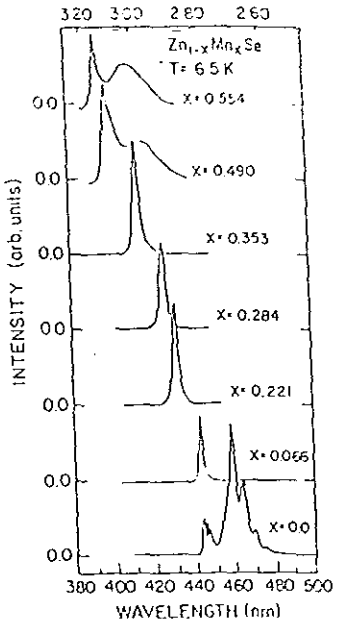

Fig. 3.3. PL spectra of $Zn_{1-x}Mn_xSe$ for x = 0 to 0.554 at T = 6.5 K [1].

Here the highest energy feature is taken as a good measure of E_g. At x = 0.066 the band-edge PL consists of only one peak, which is slightly red shifted from the highest energy feature seen in pure ZnSe. With the incorporation of still more Mn, the band-edge PL broadens and becomes less intense.

Although the general trend of the band-edge PL energy is an increase with increasing Mn concentration, there is a deviation from this trend at x = 0.066. There is a notable scatter in the data points for $0.20 \leq x \leq 0.30$. Above x = 0.30 the dependence of E_g on x appears linear (see fig. 3.4). Measurements taken at 77 K of the band-edge PL reveal the same trends (i.e. nonlinearities, scatter in data, etc.) as at 6.5 K. The respective positions are, however, shifted to lower energies, reflecting the narrowing of the band gap with increasing temperature.

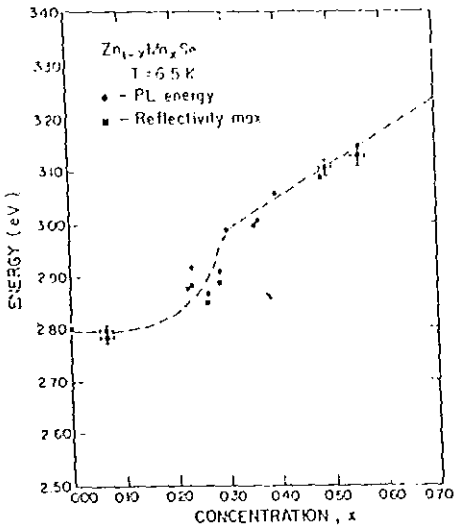

Fig. 3.4. Energy versus Mn mole fraction X in $Zn_{1-x}Mn_xSe$ of the band-edge photoluminescence peak (●) and reflectivity maximum (■) at 6..5 K [1].

Photoluminescence measurements of the band-edge feature for three of these samples were made over a temperature range from 6.5 to 250 K. The results presented in fig. 3.5 demonstrate that at high temperatures a linear closure of the band gap with temperature occurs. A deviation from the normal semiconductor behavior is present at low temperatures in samples with high Mn mole fraction: an extrablue shift of the band-edge with decreasing temperature is seen.

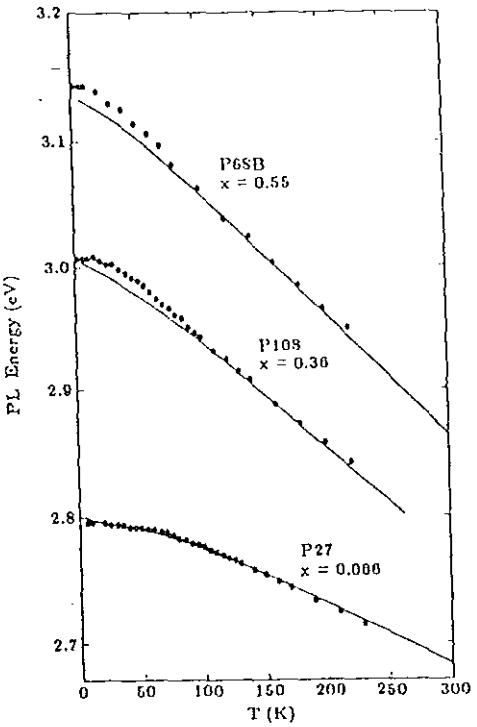

Fig. 3.5. Temperature dependence of PL peak for three Mn concentrations. The lines are theoretical fits [1].

According to Allen and Cardona [10], the optical band gap ' E_g^{0pt} ' of a crystalline tetrahedrally coordinated semiconductor depends on the temperature due to two different mechanisms. There is an explicit mechanism caused by the electron-phonon coupling and leading to an approximately linear red shift of the band gap for temperatures above the Debye temperature. The implicit mechanism is connected with the thermal lattice expansion and has a somewhat smaller effect than the explicit mechanism. For elevated temperatures both effects lead to a red shift of the gap that can be approximated by

$$E_g^{opt}(\mathrm{T}) = E_g^{opt}(0) - \gamma^{opt} T \qquad (3.1)$$

where γ^{opt} is determined from the slope of the curve $E_g^{opt}(0)$ against temperature T [11].

Since the variation of the band gap of $Zn_{1-x}Mn_xSe$ crystal with Mn concentration (x) is negligible for $x \leq 0.016$, eq. (3.1) can be applied to see the temperature dependence of the band gap of this crystal.

3.3 Energy transfer between free excitons and the 3d-electrons of Mn^{2+} in $Cd_{1-x}Mn_xS$

Wedemeyer et al. [12] gave experimental evidence of the energy transfer by excitons in $Cd_{1-x}Mn_xS$ ($x = 10^{-4}$) crystal in the spectral range of free excitons and monitored the $^4T_1 \rightarrow {}^6A_1$ emission of Mn^{2+} in the temperature range from T = 4.2 K to T = 60 K.

The identification of free excitons is supported by the different polarization behavior of the A_1, B_1 and C_1 exciton maxima of the excitation spectra at low excitation intensities due to the hexagonal structure of the crystal. The A_1, B_1 and C_1 excitons shift to lower energies as the band gap decreases when the temperature increases from T = 5 K to 30 K. The intensity dependence of the exciton peaks show the characteristic fingerprint of energy transfer. At low intensities of excitation (5 W/cm^2) pronounced A_1, B_1 and C_1 exciton peaks are observed. With increasing excitation intensity (5 kW/cm^2) the maxima of the excitation spectra disappear, and at the same energies excitation minima within a broad background appear which indicate the existence of competing energy transfer mechanism (see fig. 3.6).

Within the same spectral range two channels connected with energy transfer to the Mn^{2+} are excited. One of them consists of free excitons which delivers their energy partly to the Mn^{2+}, partly to other recombination centers. The other channel, which is dominating at high excitation levels, gives its energy predominantly to the Mn^{2+}. As a consequence the energy transfer by free excitons is relatively important at low excitation levels giving rise to maxima at the excitonic energies. At high excitation levels, however, the part of energy transferred not to Mn^{2+} is predominant leading to minima at the excitonic energies.

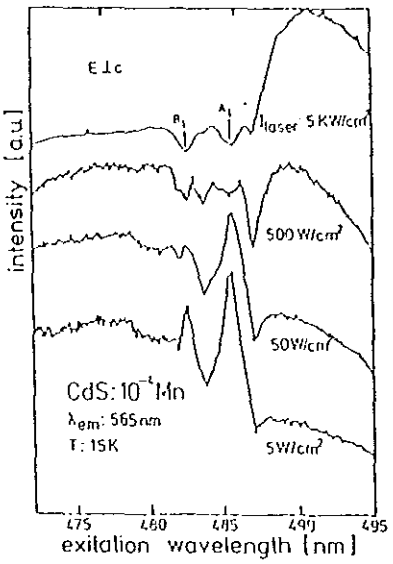

Fig. 3.6. Excitation spectra of the emission $^4T_1 \rightarrow {}^6A_1$ of $Cd_{1-x}Mn_xS$ ($x = 10^{-4}$) at different excitation intensities. The electric field of the laser is perpendicular to the C-axis of the hexagonal crystal [12].

3.4 Energy transfer between excitons and the 3d-electrons of Mn^{2+} in $Zn_{1-x}Mn_xSe$

3.4.1 Electronic transitions in the 3d-shell of Mn^{2+} ion in $Zn_{1-x}Mn_xSe$

The free Mn atom has $3d^54s^2$ configuration. Hence if one considers the $3d^5$ electrons as a part of the core, Mn is chemically divalent and thus can be used to replace a cation in the II-VI compound. A ZnSe crystal is a wide band gap (E_g = 2.82 eV for zincblende structure at T = 4.2 K) semiconductor which exists in either the cubic or hexagonal form. The transition from cubic to hexagonal $Zn_{1-x}Mn_xSe$ crystal is neglected for $x \leq 0.016$. Thus $Zn_{1-x}Mn_xSe$ crystal is stable in cubic symmetry for $x \leq 0.016$ [1].

Manganese is an efficient luminescence activator in a number of host lattices. Absorption and emission spectra of ZnSe doped with manganese have shown transitions between the $3d^5$ levels of Mn^{2+}. Due to the intra-atomic electron-electron interaction, the $3d^5$ shell of the free Mn^{2+} ion splits into 16 multiplet levels. For a Mn^{2+} ion in cubic zinc selenide crystal these 16 levels further split into 252 multiplet levels due to the crystal field of cubic

symmetry [13]. The free Mn^{2+} ion, a $3d^5$ configuration, has a ^6S ground state i.e., a symmetrical arrangement with all five spins parallel. The first excited state is a ^4G state with one spin antiparallel, and so on. The ground state is unaffected by a field of cubic symmetry, so it becomes a $^6A_1(S)$ state. The ^4G state splits into a $^4E(G)$, a $^4A_1(G)$, a $^4T_2(G)$ and a $^4T_1(G)$ level and so on.

Absorption and emission bands have been associated with electronic transitions between crystal-field split terms of the Mn^{2+} ion. One readily assigns the emissions to the lowest transition $^4T_1 \rightarrow {}^6A_1$, and the absorption bands, counting from the lower energies, to transitions from the $^6A_1$ ground state the sequence of excited states $^4T_1$, $^4T_2$, ^4E, $^4A_1$ and so on. It is possible to pump the first excited state $^4T_1(G)$, since the decay to the $^6A_1$ (S) ground state is spin forbidden and the excitation to higher excited states is followed by rapid nonradiative relaxation to the $^4T_1$ (G) level (see fig. 3.7).

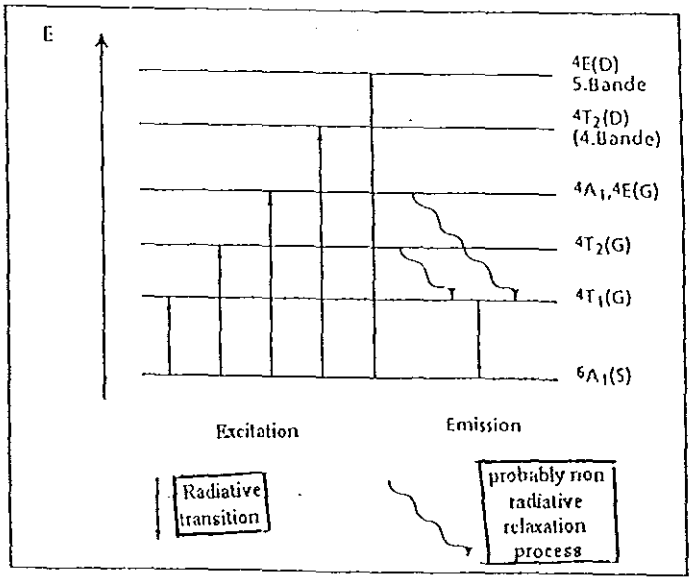

Fig. 3.7. Internal transitions of Mn^{2+} [14].

3.4.2 Energy transfer between excitons and the 3d-electrons of Mn^{2+} in $Zn_{1-x}Mn_xSe$

Stutenbaumer et al. [2] investigated the energy transfer between free excitons, bound excitions and the 3d-electrons of Mn^{2+} in $Zn_{1-x}Mn_xSe$ crystals, grown by high pressure Bridgman method. The excitation spectra were taken with an excimer pumped dye laser and corrected with a simultaneously measured dye laser reference spectrum.

The appearance of excitation maxima in the spectral range of free and bound excitons by monitoring the internal transition $^4T_1 \rightarrow {}^6A_1$ of Mn^{2+} in $Zn_{1-x}Mn_xSe$ gives evidence of an excitonic energy transfer from free and bound excitons, respectively, into the 3d-electrons of Mn^{2+} in $Zn_{1-x}Mn_xSe$. A broad excitation structure appears at the energy of bound excitons at E = 2.7915 eV. The maximum at higher energies is due to excitation of the $^4T_1 \rightarrow {}^6A_1$ Mn^{2+} transition via conduction band states and the states of free exciton. The excitation maxima at E = 2.81 eV appears within the spectral region of the band gap energy.

The excitation spectra of $Zn_{1-x}Mn_xSe$ in the range of the free excitons is markedly influenced by the Mn concentration (x). For $x > 10^{-4}$ the fine structure of the excitation spectra at the free exciton energy disappears similar to the case of $Zn_{1-x}Mn_xS$ and $Cd_{1-x}Mn_xS$ (see fig. 3.8). This effect is due to an inhomogeneous broadening of the free exciton lines by doping the crystal with manganese. The excitation spectra for x = 0.016 [fig. 3.8 curve (a)] has a pronounced maximum at E = 2.68 eV. The excitation spectrum of the $^4T_1 \rightarrow {}^6A_1$ emission band in this spectral region is dominated by the ^4E excitation band of Mn^{2+}. There is no temperature shift for this excitation maximum at E = 2.68 eV. The excitation maxima at higher energies, which are attributed to excitonic and conduction band states, shift to lower energies following the decreasing band gap due to the increase of temperature. For x = 0.0001 [fig. 3.8 curve (b)] no ^4E excitation band is observed but a fine structure appears at the high energy side of the bound exciton excitation maxima at E = 2.795 eV and at the free exciton energy at E = 2.799 eV.

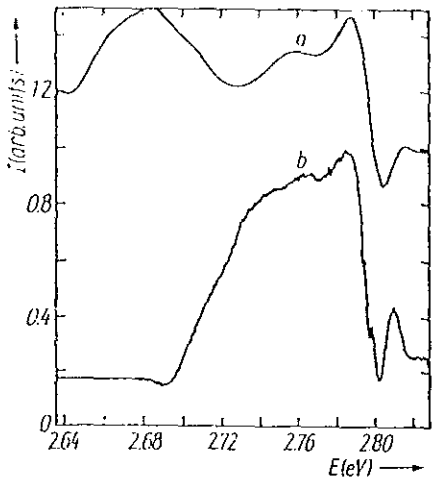

Fig. 3.8. $Zn_{1-x}Mn_xSe$ excitation spectra of crystals with different manganese concentrations. a) x = 0.016 b) 0.0001; T = 4.2 K [2].

The resonant excitation of a free exciton for x = 0.0001 leads to an enhancement of the $^4T_1 \rightarrow {}^6A_1$ emission of Mn^{2+}. The reflectivity spectra of the $Zn_{1-x}Mn_xSe$ with x = 0.0001 indicates that this enhancement is due to the energy of a transverse free excitonic polariton of the LPB which transfers its energy to the Mn^{2+} impurity after being generated by the exciting laser light at the crystal surface. Due to the great absorption coefficient at the free exciton energy the exciting light generates free excitons in a range very near to the surface. But the excitonic polariton (penetration depth $\approx$ 1μm) carries the exciting energy to the Mn^{2+} impurity. For resonant excitation of bound excitons, however, the penetration depth is some orders of magnitude greater than in the case of free excitons (see fig. 3.9). It is clear that the exciting laser light generates bound excitons at different kinds of impurities. Within their interaction range there exists a large number of manganese impurities than at the surface of the crystal. As a result the excitation of the Mn^{2+} emission via bound excitons is more pronounced than the excitation via free excitons.

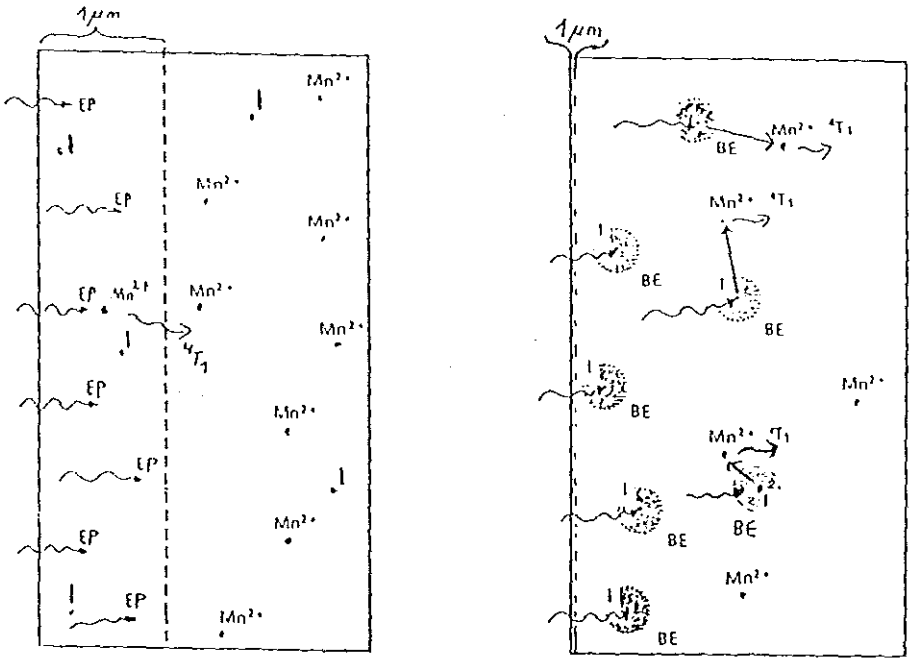

Fig. 3.9. Schematic diagram of the energy transfer of the exciton-polariton (left) bound exciton (right) to the Mn^{2+} ions in $Zn_{1-x}Mn_xSe$ [6].

4. ENERGY TRANSFER BETWEEN M-BAND AND Mn^{2+} IN $Zn_{1-x}Mn_xSe$

4.1 Curve-fitting of optical spectra

The uncertainty principle shows that those energy levels of an atom which have finite radiative lifetimes cannot be considered to be infinitely sharp. Any spectral line starting or finishing on such a level must have a corresponding frequency spread. Consequently there exists a frequency distribution of radiation intensity. In other words a radiation line has a certain shape. The shape of this line may be studied experimentally either in emission or absorption. It is described analytically by a function of frequency [15].

The two line shapes which are expected in particularly simple physical situations and which are also frequently encountered in practice are: the Lorentzian and Gaussian line shapes. Curve fitting deals with the problems of obtaining the best description of our data in terms of some theory which involves parameters whose values are initially unknown. Various fitting methods exist for parameter determination. Chi-square fitting was used for our data analyzing. The excitation structure of Mn^{2+} and DAP emissions in $Zn_{1-x}Mn_xSe$ reveal the same fine structure within the excitonic spectral range. The line shape of the excitation spectra of Mn^{2+} and DAP emissions in $Zn_{1-x}Mn_xSe$ crystals, on which our data are based, is said to be Lorentzian. This follows from the observed fact that the Lorentzian curve fits best to our excitation spectra.

4.2 Data analyzing

The line shape of our excitation spectra is given by the Lorentzian curve

$$I(x) = \frac{2AW}{\pi} \frac{1}{4(x - x_c)^2 + W^2} + y_o \qquad (4.1)$$

where the parameters: A = total area under the curve

x_c = center of the peak

W = width of the peak at half height, and

y_o = offset

This curve is symmetric with respect to the frequency ' x_c ' and has a maximum intensity at this frequency. The area under this curve is equal to the total intensity ' A ' of the emitted line. The line width is the frequency interval ' W ' between the points at which the radiation intensity drops to half of its maximum value.

The mathematical procedure for chi-square fitting of this Lorentzian curve is not only tedious, but also identical in principle for all sets of data; so it is well worth using a computer program to perform it as far as we are going to be involved in doing it more than a couple of times. The fitting was done using the Microcal Origin Program on a personal computer. Since there are two excitation peaks in the region of interest of our excitation spectra, we choose multiple Lorentzian for chi-square fitting to analyze these spectra. Using the Microcal Origin Program, when we select multiple Lorentzian for fitting and specify the number of peaks and centers of these peaks, the computer displays the chi-square value and the above parameters for each peak (see fig. 4.1). In this fitting procedure a number of trials are done

to each of our excitation spectra out of which the one with the least possible chi-square value is chosen for the best fitting. The same fitting procedures apply for the excitation spectra of both Mn^{2+} and DAP emissions in $Zn_{1-x}Mn_xSe$.

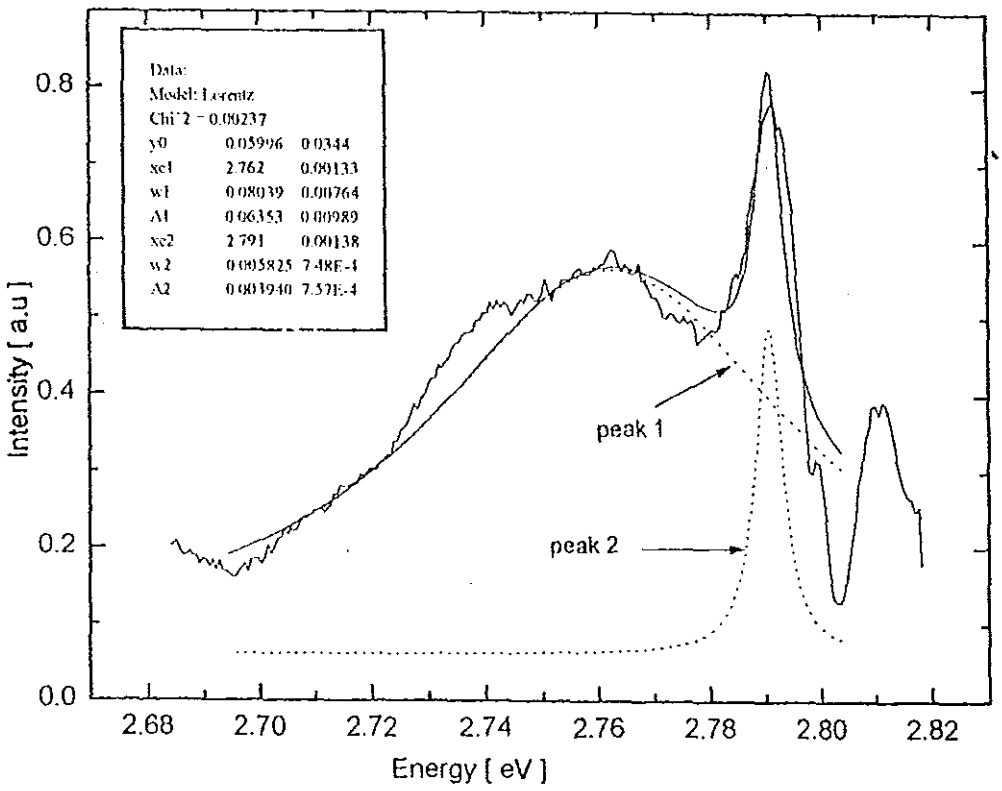

Fig. 4.1. Fitting parameters of the excitation spectra of Mn^{2+} emission in $Zn_{1-x}Mn_xSe$.

4.3 Types of spectra

This work is based on the excitation spectra of the $^4T_1 \rightarrow {}^6A_1$ emission of Mn^{2+} and DAP emission of $Zn_{1-x}Mn_xSe$ crystals from the data by H. Zuber [6]. In an excitation experiment the detector is set at a fixed energy while the energy of the exciting laser is tuned.

The first part is based on the data obtained from the excitation spectra of the $^4T_1 \rightarrow {}^6A_1$ emission of Mn^{2+} in $Zn_{1-x}Mn_xSe$ crystals, and the dependence of this spectra on the crystal temperature, Mn concentration and the intensity of the exciting laser. The second part is based on the data obtained from the excitation spectra of DAP emission in $Zn_{1-x}Mn_xSe$

crystals, and the dependence of this spectra on the crystal temperature and the intensity of the exciting laser.

For the temperature dependence of excitation spectra of both the $^4T_1 \rightarrow {}^6A_1$ emission of Mn^{2+} and DAP emission; the exciting laser intensity and Mn concentration are kept constant, while the temperature of the crystal is varying, and the excitation energies corresponding to the peaks of the M-band and bound exciton band (BE-band) are taken for different temperatures. The corresponding area and the full width at half maximum (FWHM) of each peak at different temperatures are also taken.

For the intensity dependence of excitation spectra of both the $^4T_1 \rightarrow {}^6A_1$ emission of Mn^{2+} and DAP emission; the temperature of the crystal and Mn concentration are kept constant, while the intensity of exciting laser is varying, and the excitation energies corresponding to the peaks of the M-band and the BE-band are taken for different exciting laser intensities. The corresponding area and the FWHM of each peak at different intensities are also taken.

For the Mn concentration dependence of excitation spectra of the $^4T_1 \rightarrow {}^6A_1$ emission of Mn^{2+} in $Zn_{1-x}Mn_xSe$ crystals; the temperature of the crystals and the intensity of the exciting laser are kept constant, while the Mn concentration is varying, and the excitation energies corresponding to the peaks of the M-band and the BE-band are taken for different concentrations. The corresponding area and the FWHM of each peak at different concentrations are also taken.

4.4 Tables and their figures

4.4.1 Contents of tables

Table. 4.1. Temperature dependence of the excitation spectra for Mn emission (2.13 eV) in $Zn_{1-x}Mn_xSe$ crystal at $x = 10^{-4}$, $I_{Laser} = 7\ 0\ W/cm^2$.

The data of this table are taken from the chi-square fitting parameters of the excitation spectra of the $^4T_1 \rightarrow {}^6A_1$ emission of Mn^{2+} in $Zn_{1-x}Mn_xSe$ crystal at different temperatures.

The first row contains the file names, the second row contains the temperatures of the crystal in Kelvin scale, the third and the fourth rows contain the centers of peak 1(M-band) and their corresponding errors in eV respectively, the fifth row contains the areas under peak 1 (A_1), the sixth and the seventh rows contain the centers of peak 2 (BE-band) and their corresponding errors in eV respectively, the eighth row contains the areas under peak 2 (A_2), the ninth row contains the chi-square values for the fitting, the tenth and the eleventh rows contain the band gap energies in eV taken from our excitation spectra (E_g) from the data by H. Zuber and from the photoluminescence measurements (E_g / PL) by R. B. Bylsma et al. [1] respectively, and the last row contains the ratios of areas under the two peaks (A_1/A_2).

Table 4. 2. Temperature dependence of the excitation spectra for DAP emission (2.67 eV) in $Zn_{1-x}Mn_xSe$ crystal at $x = 10^{-4}$, $I_{Laser} = 75\ W/cm^2$.

The data of this table are taken from the chi-square fitting parameters of the excitation spectra of DAP emission in $Zn_{1-x}Mn_xSe$ crystal at different temperatures.

The first row contains the file names, the second row contains the temperatures of the crystal in Kelvin scale, the third and the fourth rows contain the centers of peak 1 and their corresponding errors in eV respectively, the fifth row contains the areas under peak1(A_1),

the sixth and the seventh rows contain the centers of peak 2 and their corresponding errors in eV respectively, the eighth row contains the areas under peak 2 (A_2), the ninth row contains the chi-square values for the fitting, the tenth row contains the band gap energies in eV, and the last row contains the ratios of areas under the two peaks (A_1/A_2).

Table 4.3. Intensity dependence of the excitation spectra for Mn emission (2.13 eV) in $Zn_{1-x}Mn_xSe$ crystal at $x = 10^{-4}$, T = 4.2 K.

The data of this table are taken from the chi-square fitting parameters of the excitation spectra of the $^4T_1 \rightarrow {}^6A_1$ emission of Mn^{2+} in $Zn_{1-x}Mn_xSe$ crystal at different exciting laser intensities.

The first row contains the file names, the second row contains the intensities in W/cm^2 of the exciting laser, the third and the fourth rows contain the centers of peak 1 and their corresponding errors in eV respectively, the fifth row contains the areas under peak 1(A_1), the sixth and the seventh rows contain the centers of peak 2 and their corresponding errors in eV respectively, the eighth row contains the areas under peak 2 (A_2), the ninth row contains the chi-square values for the fitting, the tenth row contains the band gap energies in eV, and the last row contains the ratios of areas under the two peaks (A_1/A_2).

Table 4.4. Intensity dependence of the excitation spectra for DAP emission (2.67 eV) in $Zn_{1-x}Mn_xSe$ crystal at $x = 10^{-4}$, T = 5 K.

The data of this table are taken from the chi-square fitting parameters of the excitation spectra of DAP emission in $Zn_{1-x}Mn_xSe$ crystal at different exciting laser intensities.

The first row contains the file names, the second row contains the intensities in W/cm^2 of the exciting laser, the third and the fourth rows contain the centers of peak 1 and their

corresponding errors in eV respectively, the fifth row contains the areas under peak 1(A_1), the sixth and the seventh rows contain the centers of peak 2 and their corresponding errors in eV respectively, the eighth row contains the areas under peak 2 (A_2), the ninth row contains the chi-square values for the fitting, the tenth row contains the band gap energies in eV, and the last row contains the ratios of areas under the two peaks (A_1/A_2).

Table 4.5. Concentration dependence of the excitation spectra for Mn emission (2.13 eV) or DAP emission (2.67 eV) if x = 0, in $Zn_{1-x}Mn_xSe$ crystals at T = 5 K, I_{Laser} = 4 W/cm^2.

The data of this table are taken from the chi-square fitting parameters of the excitation spectra of the $^4T_1 \rightarrow {}^6A_1$ emission of Mn^{2+} in $Zn_{1-x}Mn_xSe$ crystals at different Mn concentrations.

The first row contains the file names, the second row contains the Mn concentrations of the $Zn_{1-x}Mn_xSe$ crystals, the third and the fourth rows contain the centers of peak 1 and their corresponding errors in eV respectively, the fifth row contains the areas under peak 1 (A_1), the sixth and the seventh rows contain the centers of peak 2 and their corresponding errors in eV respectively, the eighth row contains the areas under peak 2 (A_2), the ninth row contains the chi-square values for the fitting, the tenth row contains the band gap energies in eV, and the last row contains the ratios of areas under the two peaks (A_1/A_2).

4.4.2 Tables

Table 4.1. Temperature dependence of Mn emission (2.13 eV)

[$x = 10^{-4}$, $I_{Laser} = 70$ W/cm^2]

File name	ZSM69	ZSM68	ZSM67	ZSM66	ZSM65	ZSM70
Temperature (K)	5	20	40	60	80	100
Center of peak 1 [M-band] (eV)	2.762	2.760	2.758	2.723	2.715	2.692
Error in peak 1 (eV)	+/-0.00182	+/-0.00155	+/-0.0017	+/-0.00994	+/-0.00655	+/-0.00512
Area under peak 1 [A_1]	0.1685	0.1684	0.1611	0.3242	0.4659	0.2988
Center of peak 2 [BE-band] (eV)	2.790	2.789	2.787	2.779	2.771	2.775
Error in peak 2 (eV)	+/-0.00233	+/-0.00221	+/-0.0023	+/-0.00523	+/-0.00241	+/-0.0021
Area under peak 2 [A_2]	0.005137	0.005108	0.005319	0.08749	0.1114	0.1689
Chi^2	0.00463	0.00471	0.00547	0.00646	0.00265	0.00075
E_g (eV)	2.811	2.810	2.807	2.805	2.800	2.794
E_g / PL (eV) x = 0.066	2.795	2.795	2.793	2.791	2.782	2.777
A_1 / A_2	32.8	33.05	30.29	3.71	4.18	1.77

Table 4.2. Temperature dependence of DAP emission (2.67 eV)

[$x = 10^{-4}$, $I_{Laser} = 7.5$ W/cm^2]

File name	ZSM60	ZSM61	ZSM62	ZSM63	ZSM64
Temperature (K)	5	20	40	60	80
Center of peak 1 [M-band] (eV)	2.757	2.758	2.755	2.753	2.752
Error in peak 1 (eV)	+/-0.00113	+/-0.00296	+/-0.0015	+/-0.00434	+/-0.0145
Area under peak 1 [A_1]	0.1123	0.08928	0.1195	0.02593	0.0221
Center of peak 2 [BE-band] (eV)	2.791	2.790	2.789	2.786	2.782
Error in peak 2 (eV)	+/-0.00136	+/-0.00203	+/-0.00124	+/-0.00142	+/-0.00227
Area under peak 2 [A_2]	0.005417	0.005535	0.006562	0.009145	0.01179
Chi^2	0.0012	0.00179	0.00143	0.00082	0.00088
E_g (eV)	2.810	2.810	2.809	2.806	2.801
A_1 / A_2	20.73	16.13	18.21	2.84	1.87

Table 4.3. Intensity dependence of Mn emission (2.13 eV)

[$x = 10^{-4}$, T = 4.2 K]

File name	MZS20	MZS21	MZS22	MZS232	MZS24
Intensity (kW / cm^2)	0.3	3	15	30	300
Center of peak 1 [M-band] (eV)	2.742	2.741	2.743	2.743	2.74
Error in peak 1 (eV)	+/-0.000592	+/-0.00122	+/-0.00163	+/-0.00162	+/-0.00561
Area under peak 1 [A_1]	0.1848	0.2379	0.1105	0.1979	0.4027
Center of peak 2 [BE-band] (eV)	2.792	2.789	2.783	2.79	2.776
Error in peak 2 (eV)	+/-0.00106	+/-0.00203	+/-0.00241	+/-0.00282	+/-0.00337
Area under peak 2 [A_2]	0.0155	0.02098	0.008682	0.01	0.02182
Chi^2	0.00077	0.00319	0.0061	0.00232	0.00155
E_g (eV)	2.811	2.811	2.811	2.811	2.811
A_1 / A_2	11.88	11.34	12.73	15.67	18.45

Table 4. 4. Intensity dependence of DAP emission (2.67 eV)

[$x = 10^{-4}$, T = 5 K]

File name	SZM19	SZM20	SZM21	SZM22
Intensity (W / cm^2)	4	40	400	4,000
Center of peak 1 [M-band] (eV)	2.755	2.759	2.76	2.746
Error in peak 1 (eV)	+/-0.00219	+/-0.00226	+/-0.00241	+/-0.00631
Area under peak 1 [A_1]	0.03677	0.05736	0.08846	0.4249
Center of peak 2 [BE-band] (eV)	2.792	2.791	2.787	2.775
Error in peak 2 (eV)	+/-0.000845	+/-0.00121	+/-0.00211	+/-0.0035
Area under peak 2 [A_2]	0.0164	0.01195	0.01123	0.02337
Chi^2	0.00149	0.00309	0.0097	0.00234
E_g (eV)	2.811	2.811	2.811	2.81
A_1 / A_2	2.24	4.8	7.88	18.18

Table 4.5. Concentration dependence of Mn emission (2.13 eV) or DAP emission (2.67 eV) if x = 0, [T = 5 K, I_{Laser} = 4 W /cm^2]

File name	ZSM92	ZSM69	ZSM74	Znse8e	ZSM86
Concentration (x)	0	0.0001	0.001	0.008	0.016
Center of peak 1 [M-band] (eV)	2.761	2.753	2.749	2.754	2.749
Error in peak 1 (eV)	+/-0.00765	+/-0.00201	+/-0.00853	+/-0.00533	+/-0.00283
Area under peak 1 [A_1]	0.07768	0.2074	0.2582	0.1656	0.1453
Center of peak 2 [BE-band] (eV)	2.786	2.79	2.789	2.782	2.786
Error in peak 2 (eV)	+/-0.000703	+/-0.00125	+/-0.000971	+/-0.00121	+/-0.00372
Area under peak 2 [A_2]	0.03218	0.01422	0.02	0.02065	0.0201
Chi^2	0.00076	0.00336	0.00152	0.00156	0.00308
E_g (eV)	2.813	2.812	2.808	2.809	2.811
A_1 / A_2	2.41	14.58	12.71	8.02	7.23

4.4.3 Descriptions of figures

Fig. 4.2. Temperature dependence of the excitation peaks for Mn emission (2.13 eV) in $Zn_{1-x}Mn_xSe$ crystal at $x = 10^{-4}$, $I_{Laser} = 7\ 0$ W/cm^2.

The data are taken from the excitation maxima of the $^4T_1 \rightarrow {}^6A_1$ emission of Mn^{2+} corresponding to the energy transfer from the M-band to Mn^{2+}, from the BE-band to Mn^{2+}, and from the energy gap to Mn^{2+} at different temperatures.

In this figure the temperature dependence of the energies of the excitation maxima corresponding to the energy transfer from the energy gap to Mn^{2+} (E_g), and from the BE-band to Mn^{2+} shows similar characteristics for the range from T = 5 K to T = 100 K; i.e., both slightly decrease with increasing temperature. But the temperature dependence of the energies of the excitation maxima corresponding to the energy transfer from the M-band to Mn^{2+} shows an abrupt drop with increasing temperature for the range from T = 40 K to T = 60 K. Here the temperature dependence of the energies of the excitation maxima corresponding to the energy transfer from the energy gap to Mn^{2+} (E_g) agrees with the results obtained using photoluminescence measurements (E_g /PL) for x = 0.066 by R. B. Bylsma *et al.* [1](see fig. 3.5).

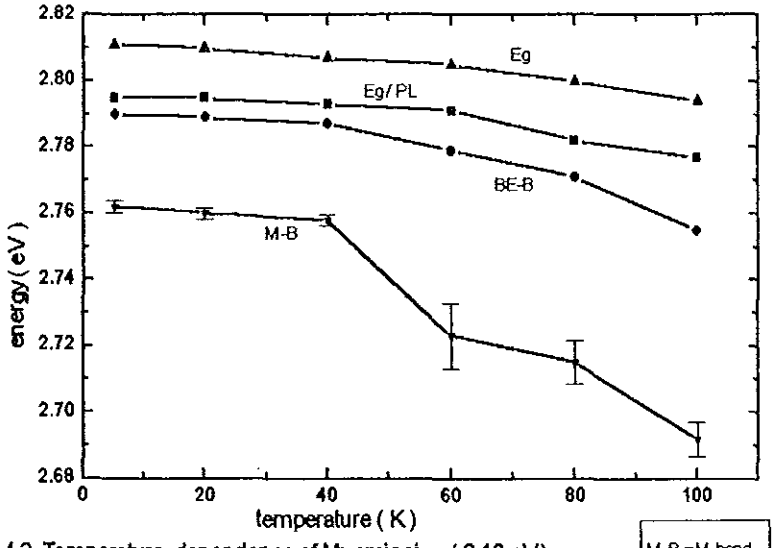

Fig. 4.2. Temperature dependence of Mn emission (2.13 eV) in $Zn_{1-x}Mn_xSe$ ($x = 10^{-4}$), $I_{Laser} = 70$ W/cm^2

Fig. 4.3. Temperature dependence of the excitation peaks for DAP emission (2.67 eV) in $Zn_{1-x}Mn_xSe$ crystal at $x = 10^{-4}$, $I_{Laser} = 7.5$ W/cm^2.

The data are taken from the excitation maxima of DAP emission corresponding to the energy transfer from the M-band to DAP, from the BE-band to DAP, and from the energy gap to DAP at different temperatures.

In this figure the temperature dependence of the energies of the excitation maxima corresponding to the energy transfer from the energy gap to DAP (E_g), from the BE-band to DAP, and from the M-band to DAP shows similar characteristics for the range from T = 5 K to T = 80 K; i.e., both slightly decrease with increasing temperature. Here the temperature dependence of the energies of the excitation maxima corresponding to the energy transfer from the M-band to DAP doesn't show an abrupt drop for the range from T = 40 K to T = 60 K unlike that of the Mn^{2+} emission (compare fig. 4.2 and 4.3).

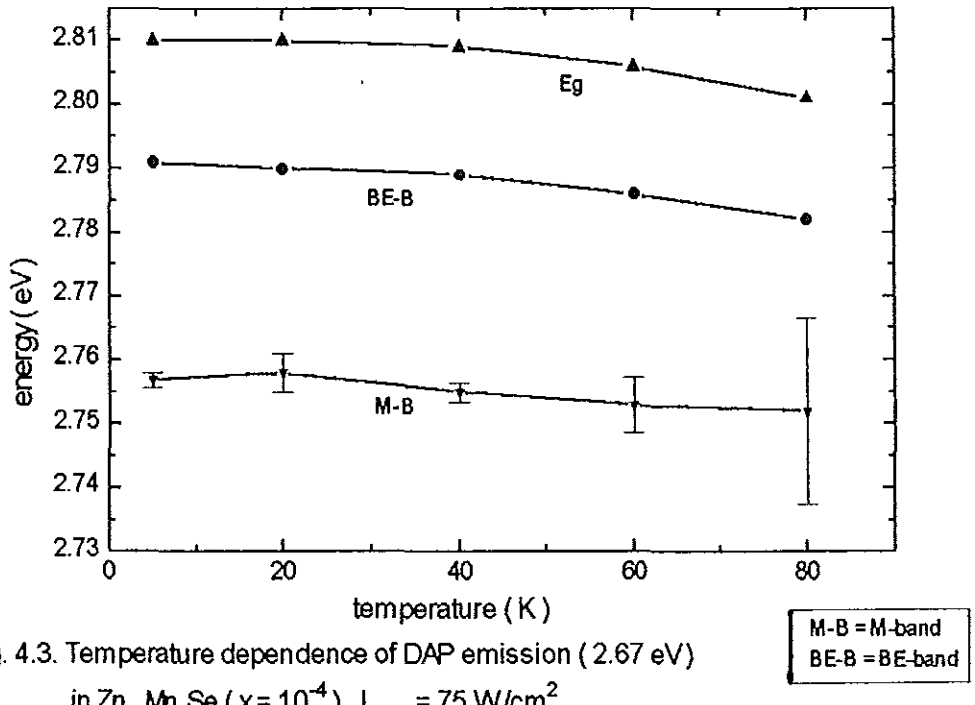

Fig. 4.3. Temperature dependence of DAP emission (2.67 eV) in $Zn_{1-x}Mn_xSe$ ($x = 10^{-4}$), $I_{Laser} = 75$ W/cm^2

Fig. 4.4. Temperature dependence of the ratio of energy transfer for Mn emission (2.13 eV) and DAP emission (2.67 eV)

The data points are the temperature dependence of the ratio of energy transfer between the M-band and Mn^{2+} to that between the BE-band and Mn^{2+} for the $^4T_1 \rightarrow {}^6A_1$ emission of Mn^{2+}; and the ratio of energy transfer between the M-band and DAP to that between the BE-band and DAP for DAP emission.

These ratios for Mn^{2+} emission and DAP emission show nearly the same characteristics for the range of temperatures from T = 5 K to T = 80 K. That is both ratios show an abrupt and rapid decrease with increasing temperature for the range from T = 40 K to T = 60 K. This implies that for the Mn^{2+} emission the areas among the excitation peaks corresponding to the energy transfer from the M-band to Mn^{2+} are getting much smaller with increasing temperature compared to the areas among the excitation peaks corresponding to the energy transfer from the BE-band to Mn^{2+} for the range of temperature from T = 40 K to T = 60 K. The same relation holds true for the areas among excitation peaks corresponding to the energy transfer from the M-band to DAP, and that from the BE-band to DAP for DAP emission.

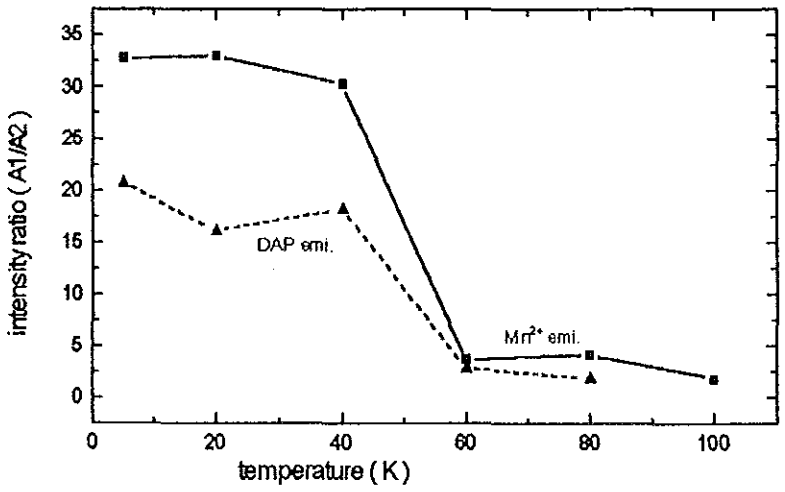

Fig. 4.4. Temperature dependence of ratio of the energy transfer between M-band & Mn^{2+} to BE-band & Mn^{2+} for Mn^{2+} emission, and that between M-band & DAP to BE-band & DAP for DAP emission

Fig. 4.5. Intensity dependence of the excitation peaks for Mn emission (2.13 eV) in $Zn_{1-x}Mn_xSe$ crystal at $x = 10^{-4}$, T = 4.2 K.

The data are taken from the excitation maxima of the $^4T_1 \rightarrow {}^6A_1$ emission of Mn^{2+} corresponding to the energy transfer from the energy gap to Mn^{2+}, from the BE-band to Mn^{2+}, and from the M-band to Mn^{2+} at different exciting laser intensities.

The energies of the excitation maxima corresponding to the energy transfer from the energy gap to Mn^{2+} (E_g) are nearly constant with increasing exciting laser intensity for the range from 0.3 to 300 kW/cm^2. From the fact that E_g decreases with increasing temperature and from the observation that E_g is constant for this crystal, it follows that the crystal temperature is nearly constant with increasing exciting laser intensity between 0.3 and 300 kW/cm^2 (see fig. 4.2 and 4.5). But the energies of the excitation maxima corresponding to the energy transfer from the BE-band to Mn^{2+}, and that from the M-band to Mn^{2+} show some fluctuations about a certain value for the range of intensities from 0.3 to 30 kW/cm^2; and slightly decrease with increasing exciting laser intensity from 30 to 300 kW/cm^2. However these observed decreases are not due to temperature changes of the crystal.

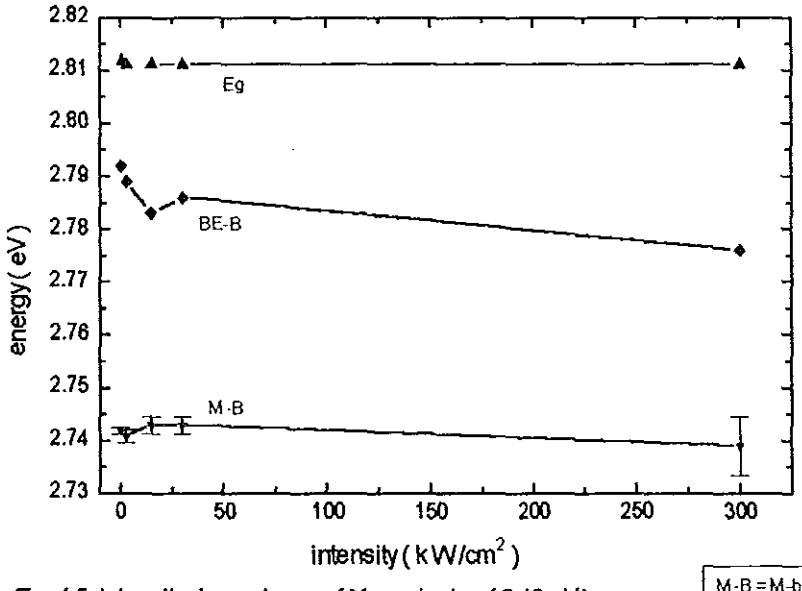

Fig. 4.5. Intensity dependence of Mn emission (2.13 eV) in $Zn_{1-x}Mn_xSe$ ($x = 10^{-4}$), T = 4.2 K

Fig. 4.6. Intensity dependence of the excitation peaks for DAP emission (2.67 eV) in $Zn_{1-x}Mn_xSe$ at $x = 10^{-4}$, T = 5 K.

The data are taken from the excitation maxima of DAP emission corresponding to the energy transfer from the energy gap to DAP, from the BE-band to DAP, and from the M-band to DAP at different exciting laser intensities.

The energies of the excitation maxima corresponding to the energy transfer from the energy gap to DAP (E_g) are nearly constant with increasing exciting laser intensity for the range from 4 to 4000 W/cm^2 similar to the results of the Mn^{2+} emission (see fig. 4.5). This implies that the crystal temperature is nearly constant with increasing exciting laser intensity for the range from 4 to 4000 W/cm^2 (see fig. 4.3 and 4.6). But both energies of the excitation maxima corresponding to the energy transfer from the BE-band to DAP and that from the M-band to DAP slightly decrease with increasing exciting laser intensity for the range from 4 to 4000 W/cm^2. However these observed decreases are not due to temperature changes of the crystal. On the average the intensity dependence of the Mn^{2+} emission is similar to that of the DAP emission (compare fig. 4.5 and 4.6).

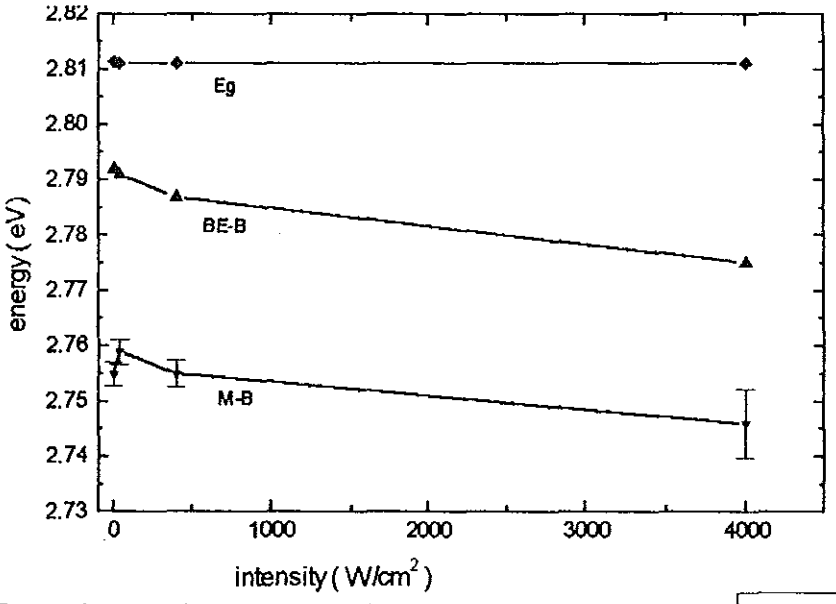

Fig. 4.6. Intensity dependence of DAP emission (2.67 eV) in $Zn_{1-x}Mn_xSe$ ($x = 10^{-4}$), T = 5 K

Fig. 4.7. Intensity dependence of the ratio of energy transfer for Mn emission (2.13 eV) and DAP emission (2.67 eV)

The data points are the intensity dependence of the ratio of energy transfer between the M-band and Mn^{2+} to that between the BE-band and Mn^{2+} for the $^4T_1 \rightarrow {}^6A_1$ emission of Mn^{2+}; and the ratio of energy transfer between the M-band and DAP to that between the BE-band and DAP for DAP emission.

For the Mn^{2+} emission the ratio of energy transfer between the M-band and Mn^{2+} to that between the BE-band and Mn^{2+} increases rapidly with increasing intensity for the range from 0.3 to 30 kW/cm^2, and then increases slightly with increasing intensity for the range from 30 to 300 kW/cm^2. The ratio of energy transfer between the M-band and DAP to that between the BE-band and DAP for DAP emission increases very much greater than that of Mn^{2+} emission with increasing intensity for the range from 4 to 4000 W/cm^2. This implies that for DAP emission the areas among the excitation peaks corresponding to the energy transfer from the M-band to DAP are getting much greater with increasing intensity compared to the areas among excitation peaks corresponding to the energy transfer from the BE-band to DAP for the range from 4 to 4000 W/cm^2.

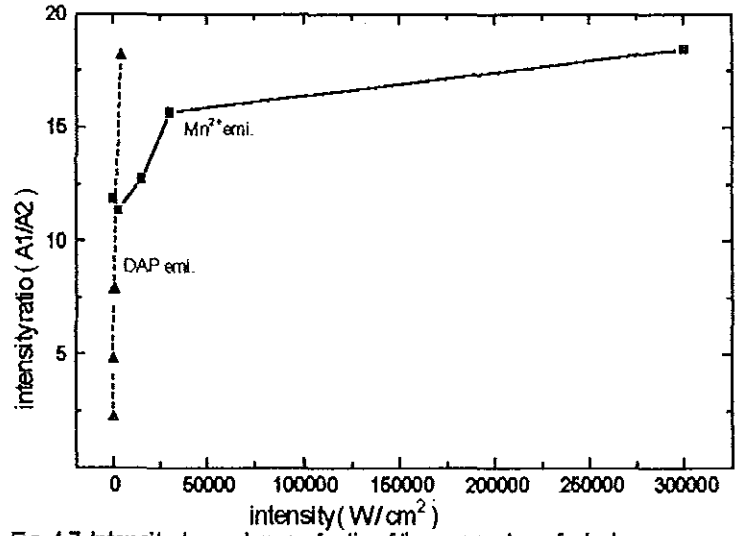

Fig. 4.7. Intensity dependence of ratio of the energy transfer between M-band & Mn^{2+} to BE-band & Mn^{2+} for Mn^{2+} emission, and that between M-band & DAP to BE-band &DAP for DAP emission.

Fig. 4.8. Concentration dependence of the excitation peaks for Mn emission (2.13 eV) in $Zn_{1-x}Mn_xSe$ at T = 5 K, I_{Laser} = 4 W /cm².

The data are taken from the excitation maxima of the $^4T_1 \rightarrow {}^6A_1$ emission of Mn^{2+} corresponding to the energy transfer from the M-band to Mn^{2+}, from the BE-band to Mn^{2+} and from the energy gap to Mn^{2+} for different Mn concentrations in $Zn_{1-x}Mn_xSe$ crystals.

Here the energies of the excitation maxima corresponding to the energy transfer from the energy gap to Mn^{2+} (E_g) slightly decrease with increasing Mn concentration for the range from $x = 10^{-4}$ to $x = 10^{-3}$, and slightly increase with increasing concentration for the range from $x = 10^{-3}$ to x = 0.016. But both energies of the excitation maxima corresponding to the energy transfer from the BE-band to Mn^{2+} and that from the M-band to Mn^{2+} fluctuate about certain values (which are different for the two peak energies) with increasing Mn concentration for the range from $x = 10^{-4}$ to x = 0.016. The point x = 0 does not belong to Mn^{2+} emission.

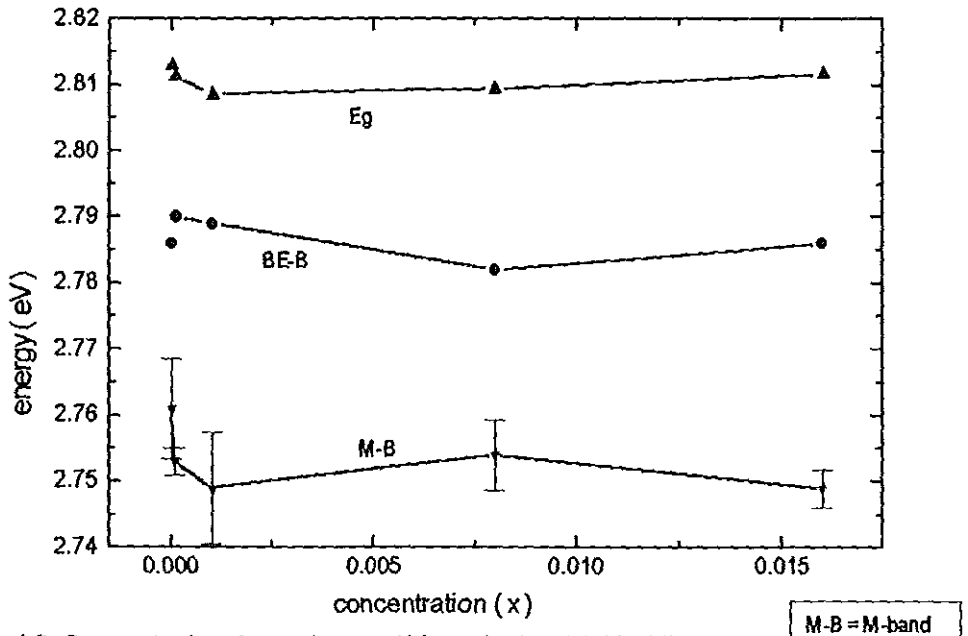

Fig. 4.8. Concentration dependence of Mn emission (2.13 eV) in $Zn_{1-x}Mn_xSe$ at T = 5 K, I_{Laser} = 4 W/cm².

Fig. 4.9. Concentration dependence of the ratio of energy transfer for Mn emission (2.13 eV) at T = 5 K , I_{Laser} = 4 W/cm² .

The data points are the Mn concentration dependence of the ratio of energy transfer between the M-band and Mn^{2+} to that between the BE-band and Mn^{2+} for the $^4T_1 \rightarrow {}^6A_1$ emission of Mn^{2+}.

These ratios slightly decrease with increasing Mn concentration for the range from $x = 10^{-4}$ to $x = 0.016$. This implies that for Mn^{2+} emission for the range of Mn concentration from $x = 10^{-4}$ to 0.016 the areas among excitation peaks corresponding to the energy transfer from the M-band to Mn^{2+} are getting much smaller with increasing Mn concentration compared to the areas among excitation peaks corresponding to the energy transfer from the BE-band to Mn^{2+}. The point $x = 0$ does not belong to Mn^{2+} emission.

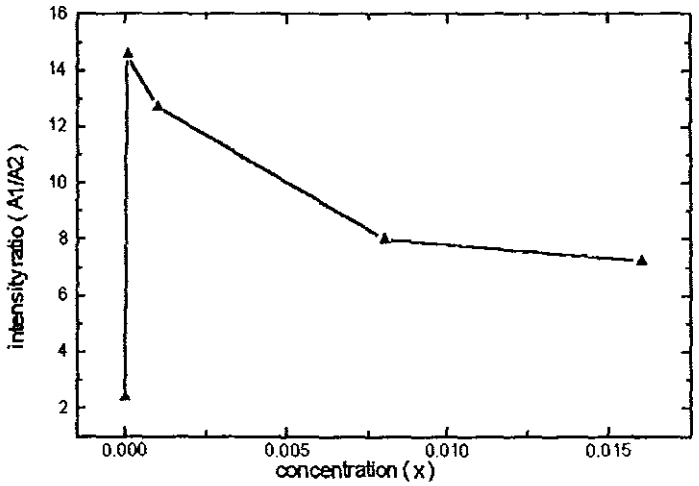

Fig. 4.9. Concentration dependence of ratio of the energy transfer between M-band & Mn^{2+} to BE-band & Mn^{2+} for Mn emission (2.13 eV) at T = 5 K, I_{Laser} = 4 W/cm²

The descriptions of the figures may be summarized as follows.

1. The temperature dependence of the excitation maxima corresponding to the energy transfer from the M-band to Mn^{2+} shows an abrupt energy shift to lower energies with increasing temperature above the temperature of 40 K unlike the temperature dependence of the energy transfer from the BE-band to Mn^{2+}.

2. The temperature dependence of the excitation maxima corresponding to the energy transfer from the M-band to DAP and that from the BE-band to DAP shows only a slight energy shift to lower energies with increasing temperature between the temperature of T = 5 K and T = 80 K.

3. For the Mn^{2+} emission, the ratio of areas among the excitation peaks corresponding to the energy transfer from the M-band to Mn^{2+} to the areas among the excitation peaks corresponding to the energy transfer from the BE-band to Mn^{2+} shows a rapid and abrupt decrease with increasing temperature from T = 40 K to T = 60. A similar temperature dependence holds for the ratio of areas among the excitation peaks corresponding to the energy transfer from the M-band to DAP to the areas among excitation peaks corresponding to the energy transfer from the BE-band to DAP for DAP emission.

4. The excitation maxima corresponding to the energy transfer from the BE-band to Mn^{2+} and that from the M-band to Mn^{2+} are not appreciably affected by changes in the intensity of exciting laser between 0.3 and 300 kW/cm^2.

5. The excitation maxima corresponding to the energy transfer from the BE-band to DAP and that from the M-band to DAP are not appreciably affected by changes in the intensity of the exciting laser between 4 and 4000 W/cm^2.

6. The ratio of areas among the excitation peaks corresponding to the energy transfer between the M-band and DAP to the areas among the excitation peaks corresponding to the energy transfer from the BE-band to DAP, for DAP emission, increases very much greater

than the corresponding ratio of areas for Mn^{2+} emission with increasing excitation intensity from 4 to 4000 W/cm^2.

7. The excitation maxima corresponding to the energy transfer from the BE-band to Mn^{2+} and that from the M-band to Mn^{2+} are not appreciably affected by changes in the Mn concentration in $Zn_{1-x}Mn_xSe$ crystals.

8. For Mn^{2+} emission, the ratio of areas among excitation peaks corresponding to the energy transfer between the M-band and Mn^{2+} to the areas among excitation peaks corresponding to the energy transfer from the BE-band to Mn^{2+} slightly decreases with increasing Mn concentration for the range from $x = 10^{-4}$ to $x = 0.016$.

5. DISCUSSION

5.1 The origin of the M-band in the excitation spectra of the Mn^{2+} impurities in $Zn_{1-x}Mn_xSe$ crystals

For temperatures between T = 5 K and T = 40 K, the excitation maxima corresponding to the energy transfer from the M-band to Mn^{2+} is slightly shift to lower energies with increasing temperature, similar to the excitation maxima corresponding to the energy transfer from the BE-band to Mn^{2+}. But when the temperature rises above T = 40 K the excitation maxima corresponding to the energy transfer from the M-band to Mn^{2+} abruptly shift to lower energies unlike the excitation maxima corresponding to the energy transfer from the BE-band to Mn^{2+}.

To account for this observed fact we took the model of the M-band that consists of a multiple of bound exciton peaks which are different from the bound excitons of the BE-band (see fig. 5.1). For temperatures between T = 5 K and T = 40 K, the energies of the excitation maxima corresponding to the energy transfer from the M-band to Mn^{2+} (~2.76 eV) are in the range of the energy levels of bound excitons. Using the M-band model, which explains the M-band as a multitude of bound exciton peaks, this implies that the excitation maxima corresponding to the energy transfer from the M-band to Mn^{2+} show similar temperature dependence with the excitation maxima corresponding to the energy transfer from the BE-band to Mn^{2+} (see fig. 4.2). That is, both maxima slightly shift to lower energies with increasing temperature. But for temperatures far above T = 40 K, for example at T = 100 K, the energies of excitation maxima corresponding to the energy transfer from the M-band to Mn^{2+} (~2.69 eV) are in the range of the ^{4}E energy level of the Mn^{2+} impurity. This implies that there is a direct energy transfer from the exciting source

to the Mn^{2+} impurities at T = 100 K.

For temperatures above T = 40 K, for example at T = 80 K, the energies of the excitation peaks of the M-band cover the range from the ^4E energy level of Mn^{2+} impurity to the energy levels of bound excitons. This implies that the excitation maxima of the M-band are due to two energy transfer channels : the direct energy transfer channel from the exciting laser source to the Mn^{2+} impurities, and the energy transfer channel from bound excitons of the M-band to the Mn^{2+} impurities.

When the temperature rises above 40 K the contribution of the direct excitation (i.e. the ^4E excitation band of Mn^{2+}) to the M-band increases with increasing temperature. This implies that the excitation maxima of the M-band abruptly shifted to lower energies with increasing temperature due to the combined effect of the ^4E excitation band of Mn^{2+} and the thermal decay of bound excitons, with less binding energy, of the M-band.

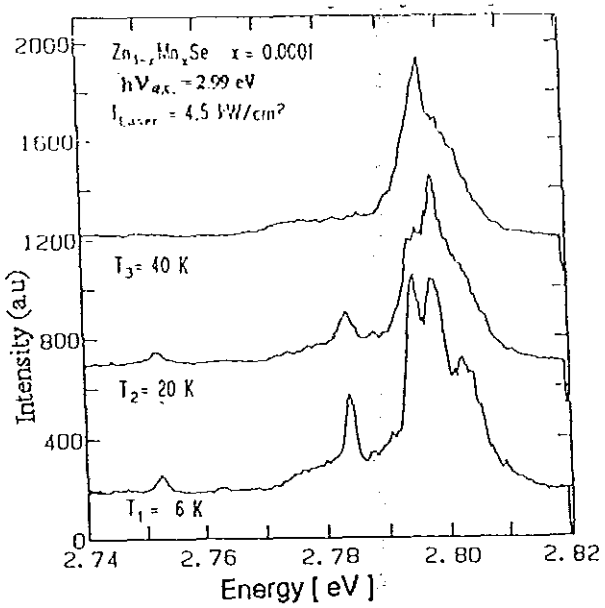

Fig. 5.1. Temperature dependence of emission spectra of $Zn_{1-x}Mn_xSe$ with $x = 10^{-4}$ after excitation into the conduction band with $h\nu_{exc} = 2.99$ eV [16].

5.2 The origin of the M-band in the excitation spectra of the DAP impurities in $Zn_{1-x}Mn_xSe$

For temperatures between T = 5 K and T = 80 K, the excitation maxima corresponding to the energy transfer from the M-band to the DAP are slightly shift to lower energies with increasing temperature similar to the excitation maxima corresponding to the energy transfer from the BE-band to DAP.

For temperatures between T = 5 K and T = 80 K, the energies of the excitation maxima corresponding to the energy transfer from the M-band to DAP (~2.76 eV) are in the range of the energy levels of bound excitons. Using the M-band model, which explains the M-band as a multitude of bound exciton peaks, this implies that the excitation maxima corresponding to the energy transfer from the M-band to DAP show similar temperature dependence with the excitation maxima corresponding to the energy transfer from the BE-band to DAP (see fig. 4.3). That is both maxima slightly shift to lower energies with increasing temperature.

5.3 Temperature dependence of competitive energy transfer channels

The excitation bands in the case of the $^4T_1 \rightarrow {}^6A_1$ emission of Mn^{2+} consist out of three competitive energy transfer channels :

1. The energy transfer channel from bound excitons of the BE-band to the Mn^{2+} impurities.
2. The energy transfer channel from bound excitons of the M-band to the Mn^{2+} impurities.
3. The direct excitation of the Mn^{2+} impurities.

The excitation bands in the case of the DAP emission consist out of two competitive energy transfer channels :

1. The energy transfer channel from bound excitons of the BE-band to DAP impurities.
2. The energy transfer channel from bound excitons of the M-band to DAP impurities.

From the work of Stutenbaumer [16] out of emission experiment it was found that some peaks of the bound exciton emission spectra of the BE-band thermally disappear at the temperature of T = 40 K (see fig. 5.1). Which means an increase for the energy transfer from the bound excitons of the BE-band to the Mn^{2+} and DAP impurities. As a result for both Mn^{2+} and DAP emissions the energy transfer of the BE-band becomes more effective with increasing temperature compared to that of the M-band for 40 K $\leq$ T $\leq$ 60 K (see fig. 4.4). A possible explanation of this fact is that a decrease of bound exciton emission due to radiative recombination results in an increase for the energy transfer to the Mn^{2+} and DAP impurities.

5.4 Intensity dependence of the energy transfer channels to the Mn^{2+} impurities

For exciting intensities between 0.3 and 300 kW/cm^2 the energies of the excitation maxima corresponding to the energy transfer from the M-band to Mn^{2+} (~2.74 eV) are in the range of bound exciton energy levels. Using the M-band model, this implies that the excitation maxima corresponding to the energy transfer from the M-band to Mn^{2+} show similar intensity dependence with the excitation maxima corresponding to the energy transfer from the BE-band to Mn^{2+} (see fig. 4.5). That is both maxima do not significantly shift in energies with increasing exciting laser intensity.

For $Zn_{1-x}Mn_xSe$ crystal the excitation maxima corresponding to the energy transfer from the BE-band to Mn^{2+} and that from the M-band to Mn^{2+} remains maxima with increasing excitation intensity. But in the case of $Cd_{1-x}Mn_xS$ crystal at low excitation intensities ($5W/cm^2$) we observe A_1 , B_1 and C_1 free exciton maxima. With increasing excitation intensity (5 kW/cm^2) the maxima of the excitation spectra disappear and at the same energies excitation minima occur [12] (see fig. 3.6).

5.5 Intensity dependence of the energy transfer channels to the DAP impurities

For exciting intensities between 4 and 4000 W/cm^2 the energies of the excitation maxima corresponding to the energy transfer from the M-band to DAP (~2.75 eV) are in the range of bound exciton energy levels. Using the M-band model, this implies that the excitation maxima corresponding to the energy transfer from the M-band to DAP show similar intensity dependence with the excitation maxima corresponding to the energy transfer from the BE-band to DAP (see fig. 4.6). That is both maxima do not significantly shift in energies with increasing exciting laser intensity.

For $Zn_{1-x}Mn_xSe$ crystal the excitation maxima corresponding to the energy transfer from the BE-band to DAP and that from the M-band to DAP remains maxima with increasing excitation intensity. But in the case of $Cd_{1-x}Mn_xS$ crystal the DAP emission shows pronounced minima in the excitation spectra at the energies of free excitons [12].

5.6 Intensity dependence of competitive energy transfer channels

The excitation bands in the case of the $^4T_1 \rightarrow {}^6A_1$ emission of Mn^{2+} at temperature T = 4.2 K consist out of two competitive energy transfer channels :

1. The energy transfer channel from bound excitons of the BE-band to Mn^{2+} impurities.
2. The energy transfer channel from bound excitons of the M-band to Mn^{2+} impurities

The excitation bands in the case of the DAP emission at temperature T = 5 K consist out of two competitive energy transfer channels :

1. The energy transfer channel from bound excitons of the BE-band to DAP impurities.
2. The energy transfer channel from bound excitons of the M-band to DAP impurities.

From the work of Stutenbaumer out of emission experiment it was found that at relatively lower laser intensities the intensity of bound exciton emission spectra of the BE-band increases with increasing exciting laser intensity (see fig. 5.2). Which means a decrease for the energy transfer from the bound excitons of the BE-band to the Mn^{2+} and DAP impurities.

As a result for Mn^{2+} emission, at relatively lower laser intensities the energy transfer through the channel from bound excitons of the BE-band to Mn^{2+} is getting less effective with increasing exciting laser intensity compared to the competitive energy transfer through the channel from bound excitons of the M-band to Mn^{2+} (see fig. 4.7).

But in the case of DAP emission, besides the decrease for the energy transfer of the BE-band there is also an increase for the energy transfer of the M-band which is due to the exciting energy of DAP is closer to the energy levels of bound excitons of the M-band. Because of these two effects, for DAP emission, the energy transfer of the M-band is getting by far more effective with increasing exciting laser intensity compared to that of the BE-band even for very low laser intensities (see fig. 4.7).

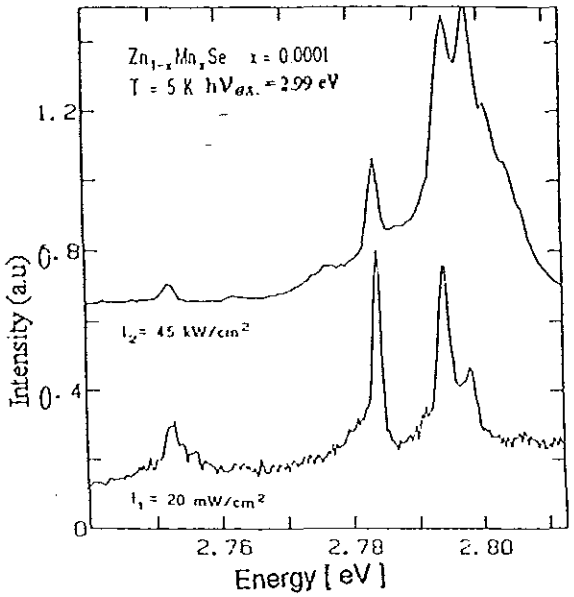

Fig. 5.2. Emission spectra of $Zn_{1-x}Mn_xSe$ crystal with $x = 10^{-4}$ and T = 5 K after excitation into the conduction band with $h\upsilon_{exc.} = 2.99$ eV. The emission spectra (above) with high excitation intensity $I_2 > 1kW/cm^2$, (below) emission spectra with low excitation intensity $I_1 < 100$ mW/cm² [16].

5.7 Concentration dependence of the energy transfer channels to the Mn^{2+} impurities in $Zn_{1-x}Mn_xSe$

For Mn concentrations (x) between $x = 10^{-4}$ and x = 0.016, the energies of the excitation maxima corresponding to the energy transfer from the M-band to Mn^{2+} (~2.75 eV) are in the range of bound exciton energy levels. Using the M-band model, this implies that excitation maxima corresponding to the energy transfer from the M-band to Mn^{2+} show similar Mn concentration dependence with the excitation maxima corresponding to the energy transfer from the BE-band to Mn^{2+}. That is both maxima do not appreciably shift in energies with increasing Mn concentration in $Zn_{1-x}Mn_xSe$ crystal (see fig. 4.8).

5.8 Concentration dependence of competitive energy transfer channels to the Mn^{2+} impurities in $Zn_{1-x}Mn_xSe$

The excitation bands in the case of the $^4T_1 \rightarrow {}^6A_1$ emission of Mn^{2+} at temperature T = 5 K consist out of two competitive energy transfer channels :

1. The energy transfer channel from bound excitons of the BE-band to Mn^{2+} impurities.
2. The energy transfer channel from bound excitons of the M-band to Mn^{2+} impurities.

From the work of Stutenbaumer out of emission experiment it was found that the intensity of the bound exciton emission of the BE-band decreases with increasing Mn concentration for $x > 10^{-4}$ in $Zn_{1-x}Mn_xSe$ crystals (see fig. 5.3). This implies that the energy transfer through the channel from bound excitons of the BE-band to Mn^{2+} is getting more effective with increasing Mn concentration, compared to the competitive energy transfer through the channel from bound excitons of the M-band to Mn^{2+} (see fig. 4.9). A possible explanation of this fact is that a decrease of bound exciton emission due to radiative recombination results in an increase for the energy transfer to the Mn^{2+} impurities.

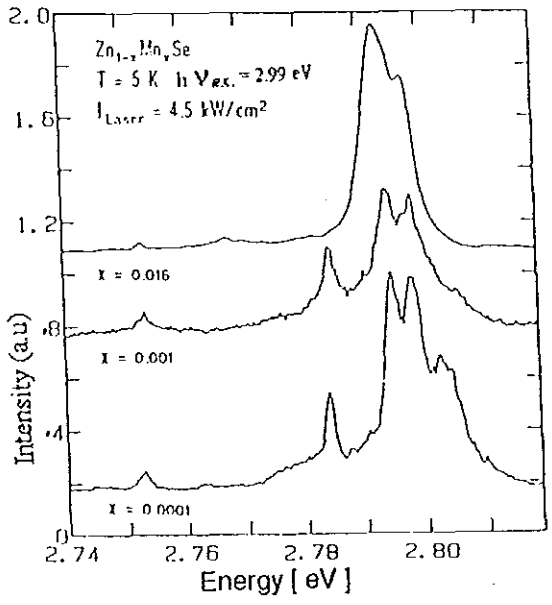

Fig. 5.3. Concentration dependence of emission spectra for $Zn_{1-x}Mn_xSe$ crystals for temperature T = 5 K after excitation into the conduction band with $h\upsilon_{exc.}$ = 2.99 eV (high excitation intensity) [16].

6. CONCLUSION

1. From the comparison of the energy transfer between the M-band and Mn^{2+} impurities with that between the BE-band and the same impurities, the M-band consists out of a multiple of bound exciton peaks. The energy transfer between these bands and the DAP impurities agrees with this M-band model.

2. The excitation maxima of the M-band in the case of the Mn^{2+} emission are due to two energy transfer channels:

-the direct energy transfer channel from the exciting photons to the Mn^{2+} impurities and

-the energy transfer channel from bound excitons of the M-band to the Mn^{2+} impurities.

3. The energy transfer from the BE-band to Mn^{2+} is getting more effective with increasing temperature compared to the competitive energy transfer from the M-band to Mn^{2+} for $40\ K \leq T \leq 60\ K$. We observe similar temperature dependence for the corresponding energy transfer between the two bands and the DAP impurities.

4. The energy transfer from the M-band to the Mn^{2+} impurities is dominating over the energy transfer from the BE-band to the Mn^{2+} impurities with increasing exciting laser intensity. We observe similar intensity dependence for the corresponding energy transfer between the two bands and the DAP impurities.

5. The energy transfer from the BE-band to the Mn^{2+} impurities is dominating over the energy transfer from the M-band to the Mn^{2+} impurities with increasing Mn concentration for $10^{-4} \leq x \leq 0.016$ in $Zn_{1-x}Mn_xSe$.

REFERENCES

[1] Bylsma R.B., Becker W.M., Kossut J., Debska U., Yoder-Short D., Phys. Rev. B33 (12), 8207 (1986)

[2] Stutenbaumer U., Gumlich H.E., Zuber H., Energy Transfer in $Zn_{1-x}Mn_xSe$ Crystals, Phys. Stat. Sol. (b) 156, 561 (1989)

[3] Klingshirn ., Proc. Int. Summer-School on Disordered Solids: Structures and Processes, Erice, Sicily, Ed. Di Bartolo B., Plenum Press (1987)

[4] Parker P., Solid State Physics Source Book, McGraw-Hill Book Company, New York (1987)

[5] Klingshirn C., Energy Transfer in Condensed Matter, Plenum Press,New York, Ed. Di Bartolo B., Nato Studies New York (1984)

[6] Zuber H., Thesis, Technical University Berlin (1990)

[7] Klingshirn C., Maier M., Blattuer G., Dean P.J., Kobbe G., J. Crystal Growth 59, 352 (1982)

[8] Broser I., Gutowski J., Riedl R., Solid State Commun. 49, 445(1984)

[9] Hoshina T., Kawai H., Jap. J. of App. Phys. 19 (2), 267-277 (1980)

[10] Allen P.B., Cardona M., Phys. Rev. B23, 1495, Phys.Rev. B24,7479 (1981)

[11] Curie D., Luminescence in Crystals,Mathuen and Co Ltd, London (1963)

[12] Wedmeyer J., Stutenbaumer U., Gumlich H.E., Journal of Luminescence 40&41, 633 (1988)

[13] Schlafer H.L., Gliemann G., Einf. in die Ligandenfeldtheorie Akad. Verl. Ges. Frankfurt (1967)

[14] Waldmann H., Thesis, Technical University Berlin (1988)

[15] Thorne A.P., Spectrophysics, J.W. Arrosmith Ltd., Bristol (1988)

[16] Stutenbaumer U., Dissertation, D83, Technical University Berlin (1990)